

DAD-A 188 055

NAVAL OCEAN SYSTEMS CENTER, SAN DIEGO, CA
SIGNAL PROCESSING STUDIES PROGRAM OPTICAL SIGNAL
AMPLIFICATION BY: H ROEHRIG, M BROWNE

1 OF 1
NOSC TD 1161 VOL 1
UNCLASSIFIED
SEP 1967

UNCLASSIFIED

END
PAGE
FILMED

NOSC

NAVAL OCEAN SYSTEMS CENTER San Diego, California 92152-5000

Technical Document 1161
Volume I
September 1987

Signal Processing Studies Program **Optical Signal Amplification**

H. Roehrig
M. Browne
San Diego State University Foundation



Approved for public release
distribution is unlimited

The views and conclusions contained in this report are those of the authors and should not be interpreted as representing the official policies, either expressed or implied, of the Naval Ocean Systems Center or the U.S. Government

NAVAL OCEAN SYSTEMS CENTER

San Diego, California 92152-5000

E. G. SCHWEIZER, CAPT, USN
Commander

R. M. HILLYER
Technical Director

ADMINISTRATIVE INFORMATION

This report was prepared by San Diego State University Foundation under contract N66001-85-D-0203 for Code 811 of the Naval Ocean Systems Center.

Released by
E.L. Rethwish, Head
Systems Architecture and
Development Branch

Under authority of
H.F. Wong, Head
Data Links Division

REPORT DOCUMENTATION PAGE

1a REPORT SECURITY CLASSIFICATION UNCLASSIFIED			1b RESTRICTIVE MARKINGS		
2a SECURITY CLASSIFICATION AUTHORITY			3 DISTRIBUTION / AVAILABILITY OF REPORT Approved for public release; distribution is unlimited.		
2b DECLASSIFICATION / DOWNGRADING SCHEDULE					
4 PERFORMING ORGANIZATION REPORT NUMBER(S)			5 MONITORING ORGANIZATION REPORT NUMBER(S) NOSC TD 1161, Volume I		
6a NAME OF PERFORMING ORGANIZATION Optical Sciences Center		6b OFFICE SYMBOL <i>(if applicable)</i>	7a NAME OF MONITORING ORGANIZATION Naval Ocean Systems Center		
6c ADDRESS (City, State and ZIP Code) University of Arizona Tucson, Arizona 85721			7b ADDRESS (City, State and ZIP Code) San Diego, CA 92152-5000		
8a NAME OF FUNDING / SPONSORING ORGANIZATION San Diego State University Foundation		8b OFFICE SYMBOL <i>(if applicable)</i> SDSU	9 PROCUREMENT INSTRUMENT IDENTIFICATION NUMBER N66001-85-D-0203		
8c ADDRESS (City, State and ZIP Code) Navy Contracts Office San Diego, CA 92182-1900			10 SOURCE OF FUNDING NUMBERS	10 SOURCE OF FUNDING NUMBERS	
			PROGRAM ELEMENT NO 62301E	PROJECT NO CM06	TASK NO DN687 623
11 TITLE (Include Security Classification) Signal Processing Studies Program Optical Signal Amplification					
12 PERSONAL AUTHOR(S) H. Roehrig, M. Browne					
13a TYPE OF REPORT Final		13b TIME COVERED FROM Jun 1986 TO Sep 1986		14 DATE OF REPORT (Year, Month, Day) September 1987	
15 PAGE COUNT 24					
16 SUPPLEMENTARY NOTATION					
17 COSATI CODES			18 SUBJECT TERMS (Continue on reverse if necessary and identify by block number)		
FIELD	GROUP	SUB-GROUP	photocathode angstroms thermionic electrons		
19 ABSTRACT (Continue on reverse if necessary and identify by block number) <p>The primary tasks associated with this contract were characterization and calibration of an RCA 8852 photomultiplier tube and a Varo image intensifier. The photomultiplier was characterized by its spectral response, absolute sensitivity, quantum efficiency, scan uniformity, dark current vs temperature, pulse-height distribution, and noise figure. The Varo intensifier was characterized by its response as a function of bias voltage both in the dark and while irradiated by an LED light source. This final report discusses the tests we performed and compares them with data in the open literature and with data obtained by means of private communication from other researchers in the field. Some tests are also discussed in the bimonthly report covering the period from June 26, 1986 to August 25, 1986.</p>					
20 DISTRIBUTION / AVAILABILITY OF ABSTRACT <input type="checkbox"/> UNCLASSIFIED / UNLIMITED <input checked="" type="checkbox"/> SAME AS RPT <input type="checkbox"/> DTIC USERS			21 ABSTRACT SECURITY CLASSIFICATION UNCLASSIFIED		
22a NAME OF RESPONSIBLE INDIVIDUAL M.S. Kvigne			22b TELEPHONE (Include Area Code) (619) 225-7936		22c OFFICE SYMBOL Code 811

UNCLASSIFIED

SECURITY CLASSIFICATION OF THIS PAGE (When Data Entered)

[Empty rectangular box for content]

UNCLASSIFIED

SECURITY CLASSIFICATION OF THIS PAGE (When Data Entered)

DETECTOR EVALUATION FOR OPTICAL SIGNALS

This report covers activities authorized under US Navy Contract Number N66001-85-D-0203 related to Task One, performed by the Optical Sciences Center from August 26, 1986, to September 30, 1986

Central to our work was the analysis of an RCA 8852 photomultiplier tube (PMT), received from Dr. Sam Green of the McDonnell-Douglas Corporation. We also worked on an image intensifier, supplied by Bill Flynt of the Varo Corporation.

For the RCA 8852, the emphasis was on:

- Quantum efficiency as a function of wavelength
- Relative responsivity as a function of position over the useful area of the photocathode
- Anode current as a function of temperature
- Dark electron pulse-height distribution

In particular, it was important to evaluate the dark current of the RCA 8852 PMT as a function of temperature. Because of its high dark current at room temperature, it is impossible to obtain single electron pulse-height distributions with our system, which is designed for a maximum event rate of $r_{ev} = 3.3 \times 10^4$ events per second. The event rate of the 8852 at room temperature and -1600 V bias is around 3×10^5 events per second.

With respect to the Varo intensifier, the emphasis was on light output (or quantum gain) as a function of the applied voltage. To better characterize this device, it was necessary to get a feel for its "dead" voltage V_0 and its "linearity" expressed by the parameter n . We approached this by determining the light output as a function of the applied voltage, both when the photocathode is in the dark and when it is illuminated by our light-emitting-diode (LED) light source.

These tests are detailed in the following paragraphs.

A. Quantum Efficiency and Absolute Sensitivity of the RCA 8852 Photomultiplier Tube

To use the RCA 8852 PMT as a reference tube, the calibration procedure had to determine its absolute spectral response, which necessitated a thorough re-examination of the calibration facility. This facility, under the direction of Dr. Richard Cromwell of Steward Observatory, consists of a light source of known output, a very stable power supply for the

lamp, a filter wheel, a set of calibrated interference filters, a set of calibrated reference photocathodes, and a data-recording system consisting of an electrometer and a HP-41 calculator to control the electrometer and gather data. The center wavelength of the filters (and hence the wavelength regions of measurement) are as follows: 298.9 nm, 313.0 nm, 350.0 nm, 380.8 nm, 406.4 nm, 425.0 nm, 497.4 nm, 550.0 nm, 650.0 nm, 750.9 nm, 795.0 nm, 853.0 nm and 901.9 nm.

From records of the calibrated photocathodes kept since 1980, we could track their degradation and select the best photocathodes to use as reference standards. The four reference photocathodes came from Hamamatsu, RCA, ITT, and Varo. In the wavelength region between 350 nm and 500 nm, we found that the photocathodes were stable to $\pm 1\%$. In the ultraviolet, the Varo tube has no appreciable response, the Hamamatsu and the ITT are stable to within 2%, and the RCA seems to have increased its response by about 8%. For wavelengths longer than 500 nm we found that all of the photocathodes except the Hamamatsu had decayed somewhat. The Varo tube had decayed substantially, the RCA tube somewhat less, and the ITT tube still less, but all three were unstable enough at the long wavelengths of interest to preclude their being considered reference standards.

The Hamamatsu was chosen as the reference photocathode; its uncertainties at the longer wavelength filters are as follows:

+0%, -10% at 901.9 nm and 853 nm
+0%, -5% at 750.9 nm and 795 nm
+0%, -3% at 650 nm
 $\pm 1\%$ at 550 nm.

Interesting to note is that in Dr. Cromwell's collection of photocathodes, every tube measured thus far over a 6.5-yr period has decayed somewhat in the longer wavelength region (with the exception of the Hamamatsu) including the most stable (a Proxitronic 3861). The worst tube (Varo #28687) has decayed 77% in 4.75 years (or 16% per year) at 901.9 nm.

We next measured the response of the RCA 8852 photocathode alone to get the absolute sensitivity. This measurement was performed both at room temperature and cooled to -50°C (this temperature is nominal, with no real way to measure it accurately; we merely wanted to compare the two modes of operation). The PMT response is shown in Fig. 1. The graph reveals two interesting facts: 1) poor response at long wavelengths and 2) a response at longer wavelengths which worsens somewhat with cooling. After correcting the measured quantum efficiency for the non-uniform response of the photocathode (averaging over the whole photocathode as discussed in Section B) the quantum efficiency at 853 nm is 1.02% uncooled and 0.54% cooled. The uncooled measurement compares favorably with that made

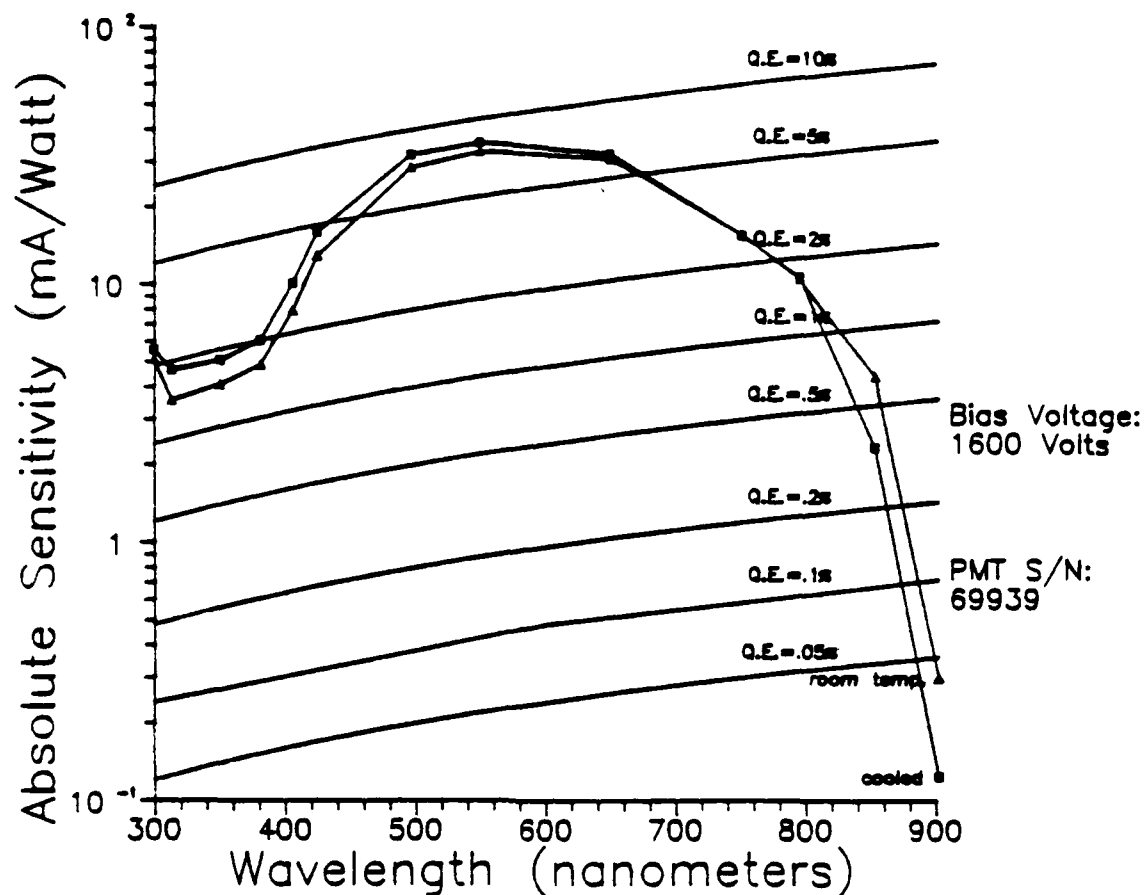


Fig. 1. Absolute sensitivity of RCA 8852 PMT measured both at room temperature and cooled.

by Dr. Sam Green in July, 1985, when he measured a quantum efficiency of 0.94%.¹ At 902 nm we measured a quantum efficiency of 0.082%. Dr. Green measured a quantum efficiency of 0.12% at a wavelength of 894 nm. Since we did not measure the photocathode uniformity at 894 nm, direct comparison of the quantum efficiency at longer wavelengths is not possible; but we feel that the rapidly decreasing tube response at longer wavelengths indicates that given Dr. Green's measurement at 894 nm, ours at 902 nm is not unreasonable.

The decreasing quantum efficiency at lower temperatures is most likely because at the longer wavelengths, photons may just have enough energy to create a photoelectron (possibly with the assistance of a phonon), and therefore lowering the device temperature will reduce the amount of phonons present, making fewer phonon-assisted transitions possible.

B. Spatial Uniformity of the Photocathode Sensitivity

When measurements of the absolute spectral response of the photomultiplier were made, we also made a one-dimensional scan through the center of the photomultiplier's

photocathode and measured the photocathode current for various wavelengths of light. The results of this test are shown in Fig. 2. Notice that the response at 4250 Å is still quite good, but as we move out toward longer wavelengths, the relative response is very non-uniform. Interesting to note is that the measurements of the tube response were made approximately across the center of the photocathode, which is also the region of least sensitivity at the longer wavelengths. This would seem to indicate that the response as given by Fig. 1 would not convey an accurate indication of the overall photocathode sensitivity, and that the overall sensitivity would be somewhat larger. To take this into account in our measurements of the quantum efficiency at longer wavelengths we assumed that the response was radially symmetric. (It is not, but this probably is not too bad an assumption.) We then averaged the response over the entire scan and also over just the region of irradiation for the quantum efficiency measurements; then we ratioed these two averages as a correction factor for the measured quantum efficiency to extrapolate the quantum efficiency as would be measured over the entire photocathode for the two wavelengths 853 and 902 nm.

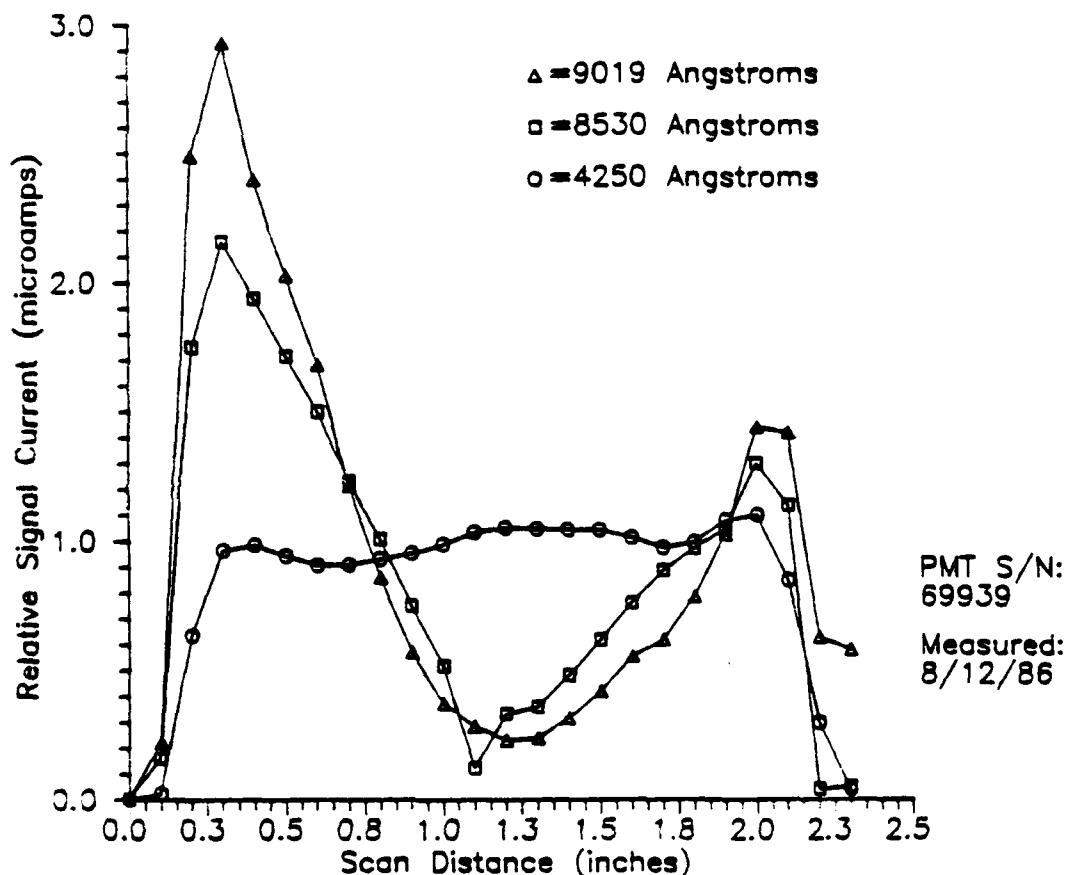


Fig. 2. Uniformity scan across the photocathode of an RCA 8852 PMT. A 0.24-in. scanning spot size was used.

Curious about the rather large variations in photocathode response as a function of position, we discussed our data with Dr. Green. It was his opinion that large variations in photocathode response are typical and are especially prevalent at longer wavelengths, where the lower energy of the photon and thus of its created photoelectron means that even the smallest defect in the photocathode will have an effect on conversion efficiency by reducing the energy of the less energetic photoelectrons so that they can no longer escape the photocathode material and become free photoelectrons.

C. PMT Anode Dark Current vs Temperature

Testing the RCA 8852 revealed that the dark current is much higher at room temperature than the dark current of the RCA 8850 (6×10^{-8} A compared to 2×10^{-11} A) at the same bias voltage of -1600 V and after both tubes had been conditioned in the dark with bias voltage on for at least 48 hr. Because of the high dark current, the 8852 was often operated at reduced temperatures by installing it in a Products for Research model TE-254-TS-RE-ND refrigerated photomultiplier housing. This housing consists of a pump/refrigeration unit and a housing unit/heat exchanger, connected by a flexible hose which carries the Freon coolant. The unit has a dial which nominally selects the temperature at the photocathode and is calibrated in six steps: 0°C , -10°C , -20°C , -30°C , -40°C , and -50°C . We were interested in measuring the reduction in dark current for a given decrease in operating temperature. The tube was biased to -1600 V and the dark current was measured at the anode using a Keithley Model 602 Electrometer. The results of this experiment are shown in Fig. 3.

As expected, there is a strong dependence of the dark current on the absolute temperature. For the specific example of -1600 V bias voltage, the anode current reduces from 4.2×10^{-8} A to about 1.5×10^{-10} A, which is more than 2 orders of magnitude. This is both expected and predictable from the Richardson equation, which gives the dependence of the electron emission of a surface on temperature (making the appropriate assumptions for the bandgap of the material).²

$$j = \frac{4\pi emk^2 T^2}{h^3} e^{((E_a - E_g)/2)/kT} \quad (1)$$

where:

- | | |
|----------------------------------|----------------------------|
| j = thermionic current density | e = electron charge |
| m = electron mass | k = Boltzmann's constant |
| h = Planck's constant | E_a = electron affinity |
| E_g = bandgap | |

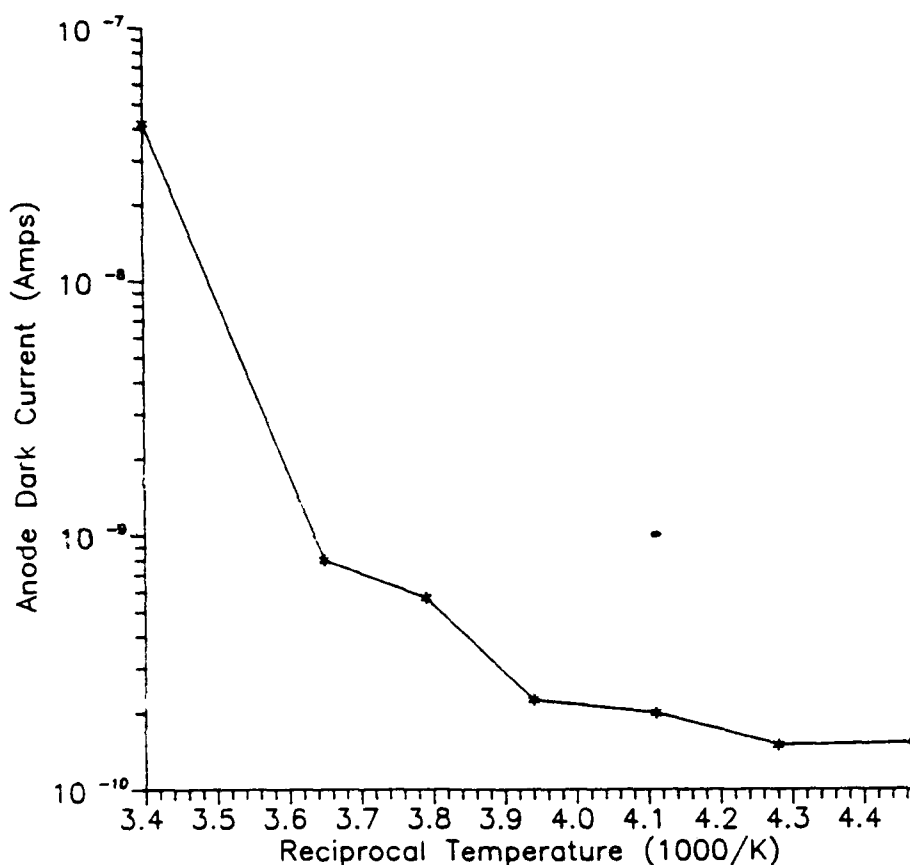


Fig. 3. Anode dark current of RCA 8852 measured as a function of temperature.

or, if the constants are given in mks units, (1) becomes

$$j = 1.2 \times 10^6 T^2 e^{((E_a - E_g)/2)/kT} \quad (2)$$

This decrease in dark current with decreasing temperature also agrees with the findings of other researchers (Dr. Richard Cromwell) and with the literature.³ An example for the latter is Fig. 16 of the RCA Photomultiplier Handbook⁴ which is reproduced in this report as Fig. 4. Our curve appears to bottom out because the temperature feedback mechanism in the cooler is not extremely reliable for the following reasons: 1) the temperature sensor makes no contact with the photomultiplier photocathode and, 2) the only indication that the cooler has actually "cooled down to temperature" is a cycling of the refrigeration unit, which could also be attributable to mechanical considerations alone (i.e., a finite on/off time to prevent frosting of the input window).

D. Single Dark Electron Pulse-Height Distributions

Single dark electron pulse-height distributions can only be made if the emission rate of dark electrons (thermionic electrons) r_{el} at the PMTs photocathode is at least an order of

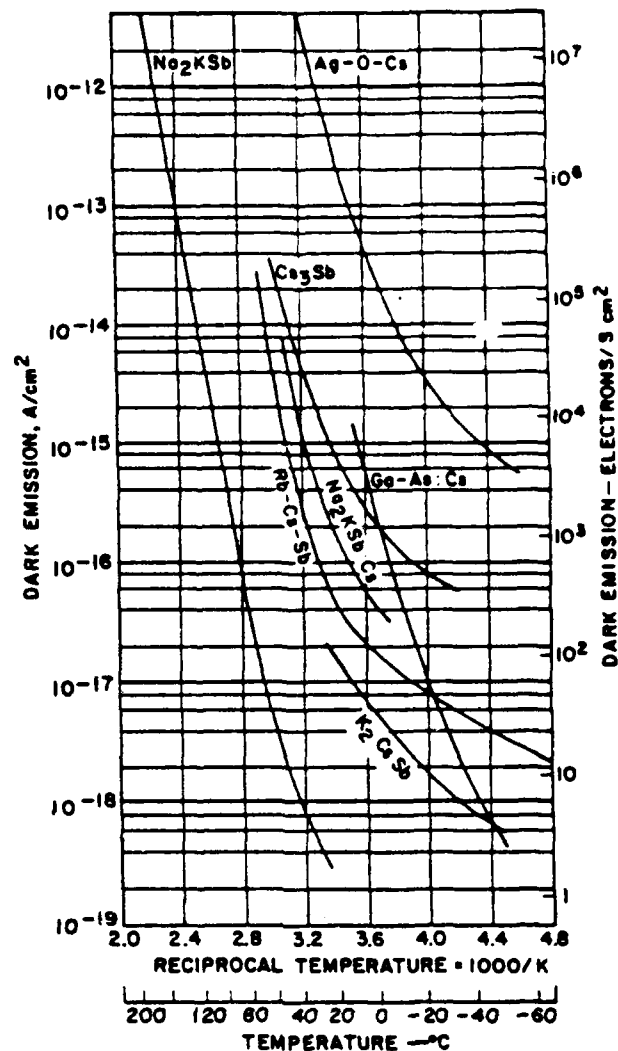


Fig. 4. Variation of thermionic-emission current density from various photocathodes used in photomultiplier tubes as a function of reciprocal temperature. Thermionic emission multiplied by the gain of the photomultiplier is a principal source of anode dark current. (Ref. 2)

magnitude (if not two orders) lower than the highest event rate r_{ev} the instrumentation can handle:

$$r_{el} \ll r_{ev} \quad (3)$$

We commonly use an integrator described in detail in the final report for Contract N66001-85-C-0118.⁵ Its shortest integration time is $t_i = 30 \mu s$ and, consequently, its highest event rate r_{ev} is $r_{ev} = 1/t_i = 1/(30 \mu s) = 3.3 \times 10^4$ events per second.

The condition of Eq. (3) can be achieved for the RCA 8852 PMT by cooling to $-50^\circ C$ (nominal). At this temperature, the anode dark current is about 2×10^{-10} A. Assuming a gain of 9×10^5 for -1600 V, (a value which can be found from the RCA data sheets on the

RCA 8852),⁶ the dark electron rate at the cathode is $r_{el} = 1.4 \times 10^3$ electrons/second. This value is easily matched by the event rate $r_{ev} = 3.4 \times 10^4$ events per second.

Figure 5 shows a single dark electron pulse-height distribution taken with the RCA 8852 at a temperature of about -50°C . It was obtained using a PMT voltage of -1600 V , a load resistor of $21.4 \text{ k}\Omega$, an integrator gain of 98647 sec^{-1} , a preamp gain setting of 500, and an MCA sensitivity of $S_{MCA} = 256 \text{ channels/volt}$. The integrator was operated in the internally triggered mode. Notice that the distribution peak is at channel number 80.

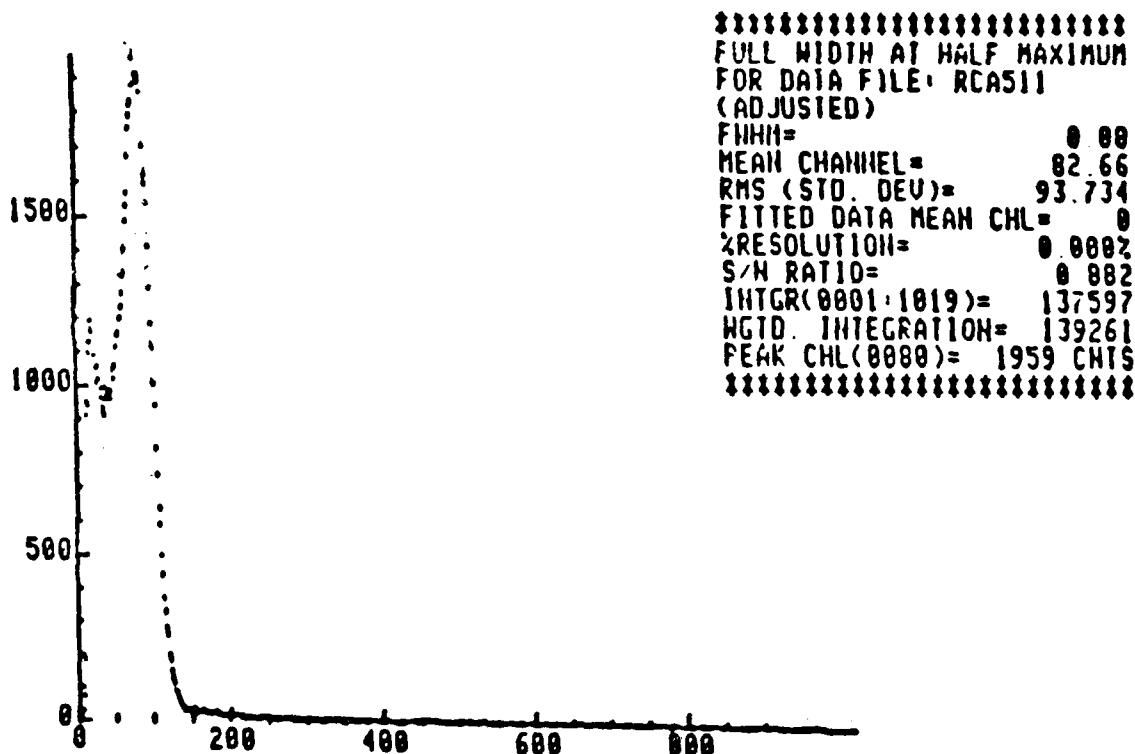


Fig. 5. Pulse-height distribution for an RCA 8852 PMT at -1600 V bias and cooled to -50°C (nominal).

The experimental setup is similar to that shown schematically in Figs. 6 and 7. Notice that the setup includes a light source (LED) which of course is not used for measuring single dark electron pulse-height distributions. Rather, it is only used if measurement of single signal electron pulse-height distributions (which incidentally should not be different from the single dark electron distributions) is desired. Figure 7 describes the operation of the integrator and provides a formula by which the photomultiplier's gain can be calculated from the characteristics of the distribution displayed by the multichannel analyzer (MCA). This equation is repeated here in a slightly modified form:

$$G = \frac{N_{ch} \cdot R_I \cdot C_I}{S_{MCA} \cdot G_A \cdot R_I \cdot e} \quad (4)$$

where:

$1/(R_I \cdot C_I)$ = "gain of the integrator" [s^{-1}]

G_A = voltage gain of the preamplifier

R_I = load resistor [Ω]

e = electronic charge [coulombs]

S_{MCA} = sensitivity of the MCA [channels/V]

N_{ch} = channel number of particular characteristic of distribution.

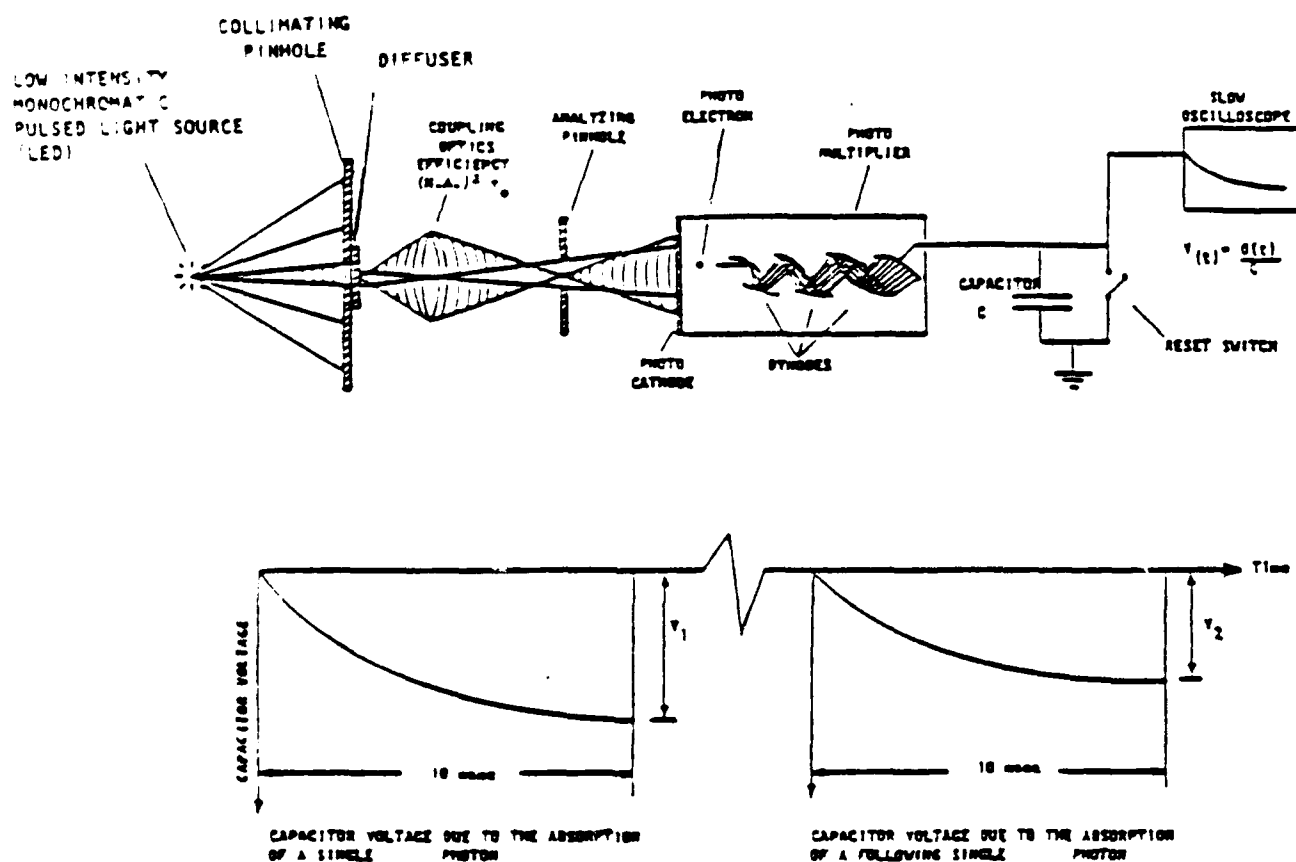


Fig. 6. Schematic illustrating the measurement of photoelectron pulse-height distribution of a photomultiplier using an analog integrator (capacitor with a reset switch) and a pulsed light source (LED).

Assuming for the moment that the distribution feature of interest is the distribution peak (one could also argue for the use of the distribution mean, weighted mean, median,

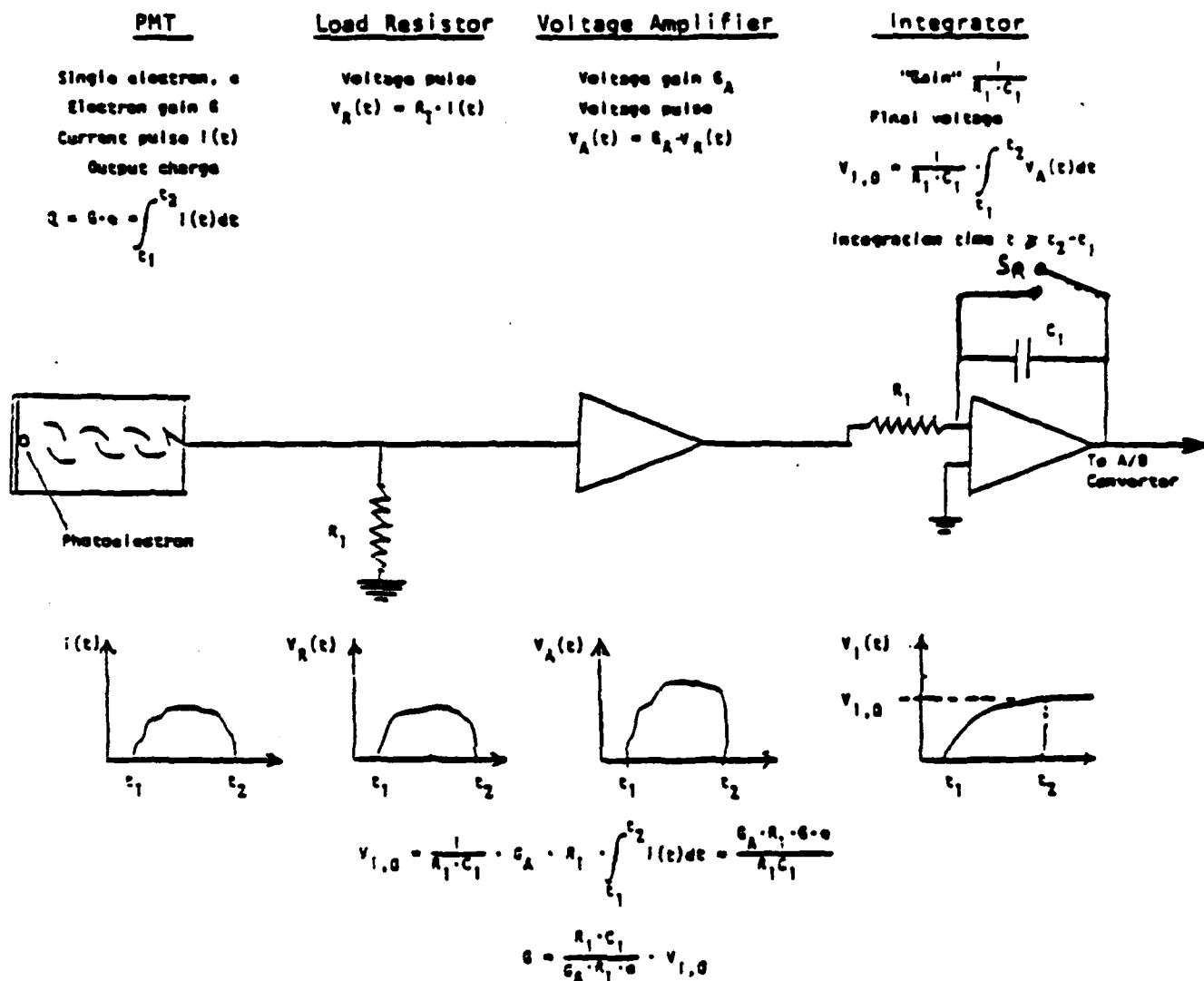


Fig. 7. The measurement of a photomultiplier's gain G from the integrator's voltage V for a PMT charge pulse attributable to one photoelectron (single electron pulse).

etc.; this subject has not been specifically addressed yet, and we are open for suggestions). the gain of the PMT is estimated to be 1.85×10^5 . This gain value compares favorably with the value of 9×10^5 , which is quoted as being typical by the RCA data sheet for the 8852.⁴

Of particular interest to this program is the determination of the noise factor, a characteristic which determines the amount of noise added by the detector (excess noise) to the noise inherent in the photon flux from the scene. As was outlined in the Final Report for Project N66001-85-C-0118,⁵ the noise factor k is found from the mean μ_2 and the

standard deviation σ_s of the single electron distribution according to:

$$k = \frac{\mu_s^2 + \sigma_s^2}{\mu_s^2} \quad (5)$$

Using the values found in the above distribution, we find a value of 2.29 for the noise factor which seems to be reasonable.

It is interesting to relate the number of counts N_{co} (total integrated counts = 139261) recorded during the duration T_e of the experiment (which was 2000 s) to the observed anode dark current i_A . Assuming that every dark electron emitted by the cathode leads to a recordable event (has enough amplitude to exceed the integrator's internal trigger threshold and therefore increment a channel in the multichannel analyzer) then the count rate r_{MCA} at the MCA should be matched by the dark electron rate r_{el} at the PMT's cathode or the dark electron rate $r_{el,A}$ at the PMT's anode divided by the PMT's gain G_{PMT} :

$$r_{MCA} = \frac{N_{co}}{T_e} = \frac{r_{el,A}}{G_{PMT}} = \frac{i_A}{G_{PMT} \cdot e} = r_{el} \quad (6)$$

For this experiment, $r_{MCA} = 68.8$ counts/s while $r_{el} = 69.3$ counts/s, an error of only 0.7%.

Finally, an attempt was made to estimate the energy resolution, which is conventionally the ratio of the FWHM to the peak channel. We found a value of 70%, which is close to the value of 60% found in the RCA 8852 data sheet.⁶

Table 1 is a listing of some pertinent performance data on the RCA 8852 as measured by us and compared with data from the data sheets or other sources.

E. Varo Intensifier Light Output and Gain vs Bias Voltage

Image intensifiers of the Generation I type operate on the principle of cathode luminescence for the generation of gain. Here electrons emitted by the cathode are accelerated to a high kinetic energy $E_{kin} = 1/2 mv^2 = eV$, where V equals the applied voltage. A major portion of this kinetic energy is used for excitation of electrons from the valence band to the conduction band of the phosphor material. Most of these excited electrons then give up their energy by returning to the valence band by means of energy levels in the forbidden band involving radiative transitions as shown schematically in Fig. 8. Unfortunately, however, not all the kinetic energy is used for the generation of light. It turns out that the electrons lose some energy in penetrating "dead" layers like the typical

Table 1. Pertinent performance data on the RCA 8852.

Quantity	Measured	From PMT Data Sheets
PMT voltage	-1600 V	—
Dark current @ -1600V	2.05×10^{-11} amps	2.0×10^{-8} amps @ 22°C
Count rate from dark current	69.3 counts/s	—
No. of counts from weighted integral	139261	—
Acquisition time	2.000 s	—
Observed count rate	68.8 counts/s	—
Peak Channel No.	80	—
Mean Channel No.	82.66	—
Standard Deviation	93.734	—
Current Gain @ -1600 V	1.85×10^6	8.5×10^5
Noise Factor (k)	2.29	1.87 - 1.94*
FWHM	56	—
Energy Resolution	70%	60%
Quantum Efficiency @ 852 nm	1.02%	0.94%*
Quantum Efficiency @ 894 nm	—	0.12%*
Quantum Efficiency @ 901 nm	0.082%	—

* From measurements made by Dr. Sam Green.¹

aluminum backing of the phosphor. This energy is characterized by the so-called dead voltage V_0 . Other losses are accounted for by the energy conversion efficiency η_{En} .

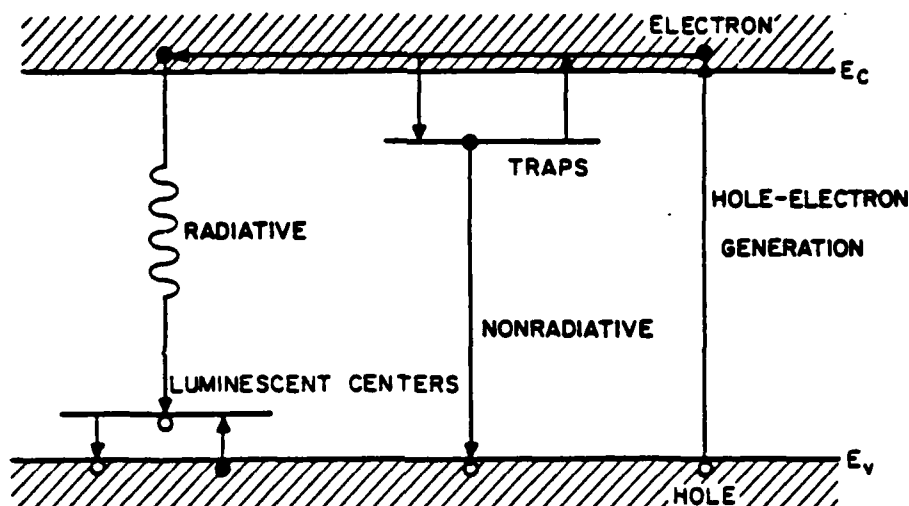


Fig. 8. Representation of radiative and nonradiative recombinations.

The number n_p of light photons emitted per photoelectron can be estimated from the effective kinetic energy $E_{kin,eff} = E_{kin} - eV_0$, the energy E_p of the emitted light photon, and the energy conversion efficiency η_{En} :

$$n_p = \eta_{En} \cdot \frac{E_{kin,eff}}{E_p} = \eta_{En} \cdot \frac{E_{kin} - eV_0}{E_p}. \quad (7)$$

Of particular interest is the dependence of η_{En} or n_p on the applied voltage. This can be estimated from the light output as a function of the accelerating voltage. The literature on cathode luminescence reports a general dependence as described in Eq. (8).⁷

$$L = k (V - V_0)^n \quad (8)$$

Here k is a constant of proportionality
 V is the applied voltage
 V_0 is the dead voltage
 n is a constant which can take on values of from 1 to 3.⁸

Figure 9 is a linear representation of Eq. (8) for $V_0 = 2$ kV and $n = 1$. Figure 10 is a double logarithmic representation of Eq. (8) for $V_0 = 3$ kV, 5 kV, and 7 kV, and for $n = 1$.

Of particular importance were the particular values of V_0 and n for the phosphor in the Varo tube.

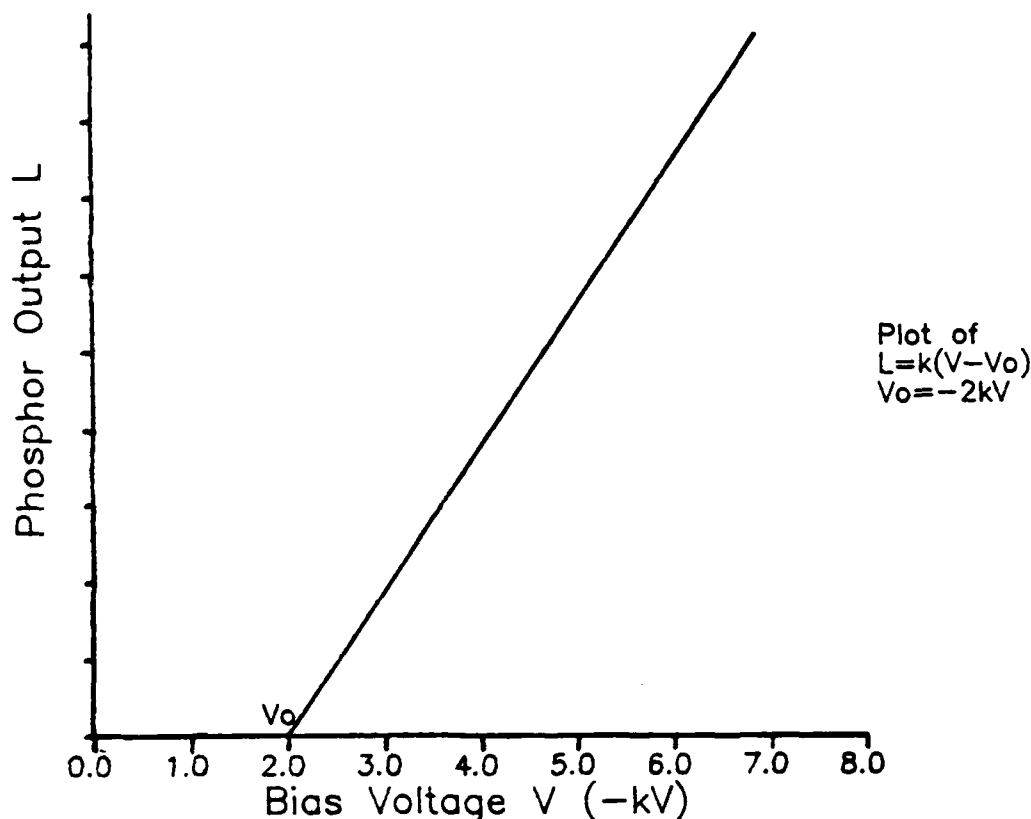


Fig. 9. Linear plot of phosphor light output as a function of applied voltage for $V_0 = -2$ kV and $n = 1$.

The experimental setup is shown schematically in Fig. 11. Notice that this is the setup which we normally use for measurements of the pulse-height distributions of image intensifiers which are basically AC type measurements. However, the system is easily modified by insertion of an electrometer into the anode circuit of the PMT to measure its DC anode current which then is a measure of the intensifier's light output.

Figure 12 shows on a log-log plot the output of the Varo image intensifier versus bias voltage, both in the dark and while irradiated. The output of the image intensifier was measured with an RCA 8850 photomultiplier tube coupled optically to the image intensifier using a high numerical aperture ($NA = 0.95$ in air) 100X microscope objective. The dark current for the photomultiplier was 2.1×10^{-11} A, and this value was subtracted from the anode current values while measuring the image intensifier. A more familiar plot may be the linear plot of the image-intensifier output vs bias voltages, which is shown in Fig. 13.

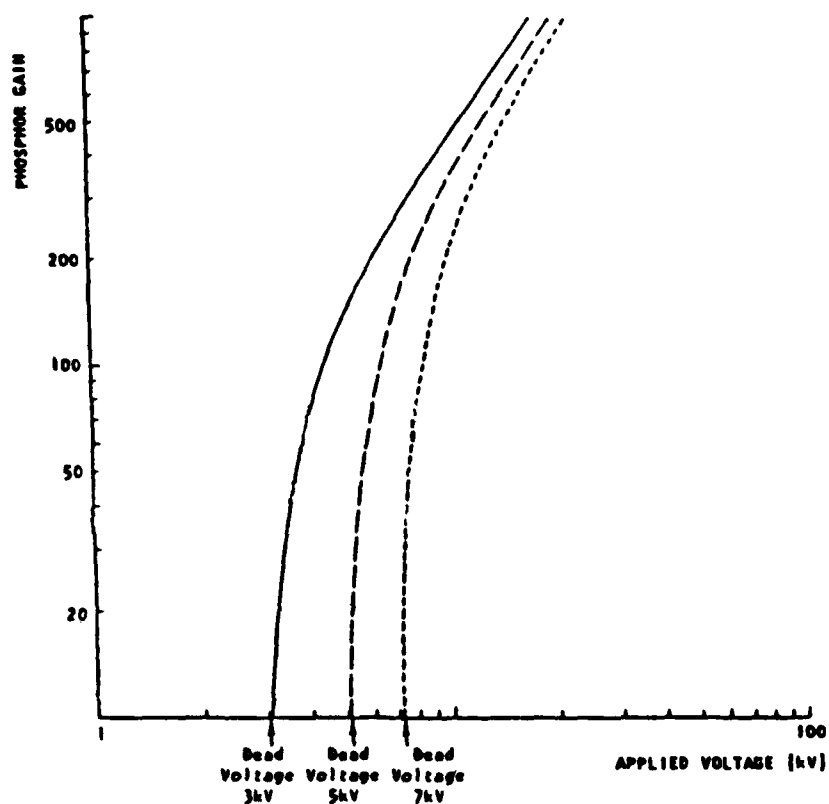


Fig. 10. Nonlinearity of P-20 phosphor gain attributable to dead voltage.

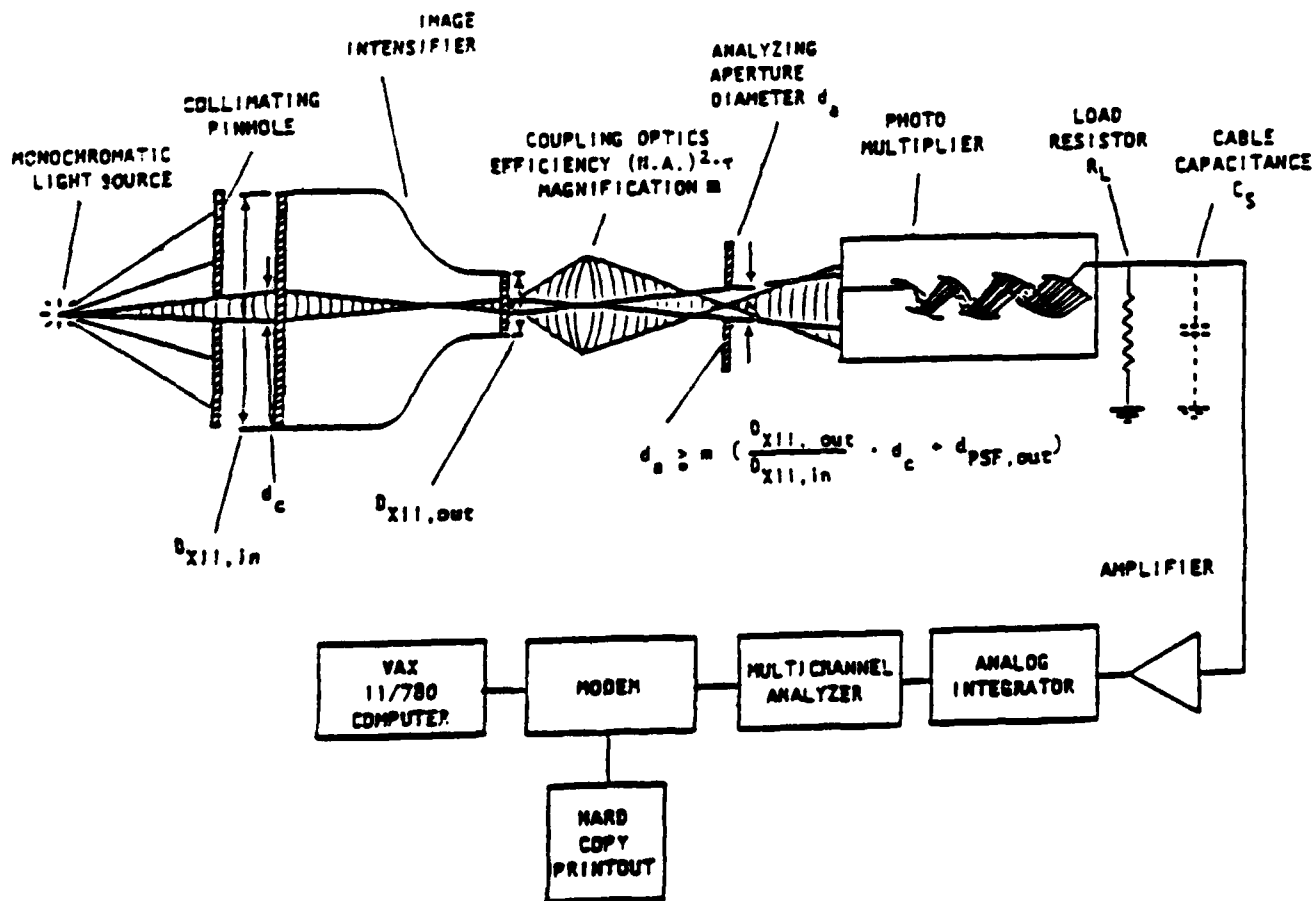


Fig. 11. Experimental setup for the measurement of single and multiple photon pulse-height distributions.

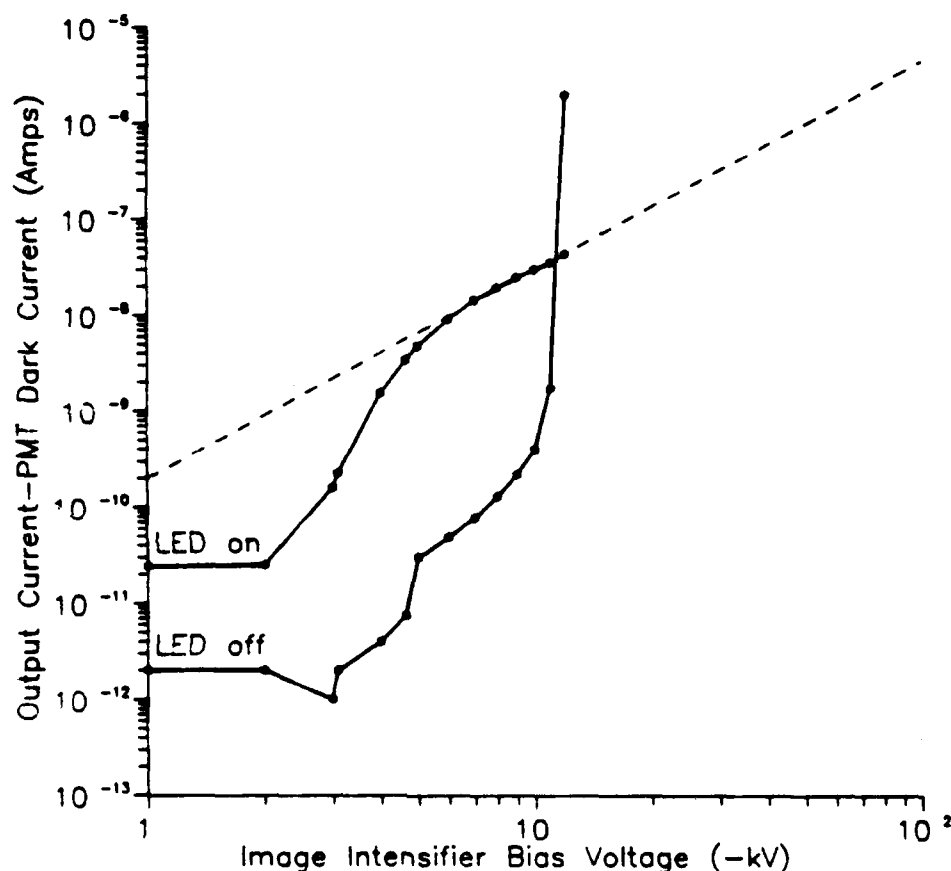


Fig. 12. Measured output of Varo image intensifier vs bias voltage.

Figure 12 is not exactly what one would expect from an image intensifier tube, particularly the measurements made at -11 and -12 kV bias voltages with the LED off.

From talking with Bill Flynt of Varo and from our own observations, we have come to the conclusion that this jump in output brightness at -11 and -12 kV is most probably attributable to a field-emission point in the diode. We have observed, and Bill Flynt has confirmed for us, that field emission points may not be stable with respect to time or position, which could be why we did not observe the field emission during the time we had the LED on.

We also observed a sort of "hysteresis" effect with the field emission point, in that it came on above a certain bias voltage but turned off at a much lower bias voltage. It is plausible that during the LED "on" experiment, this "threshold" was never exceeded but during the LED "off" experiment, it inadvertently was, and when the bias voltage was reduced, the field emission point was still glowing. The data sheets included with this image intensifier tube indicate that the tube was damaged during testing and on observing the tube at high bias voltages, bright emission points could be seen.

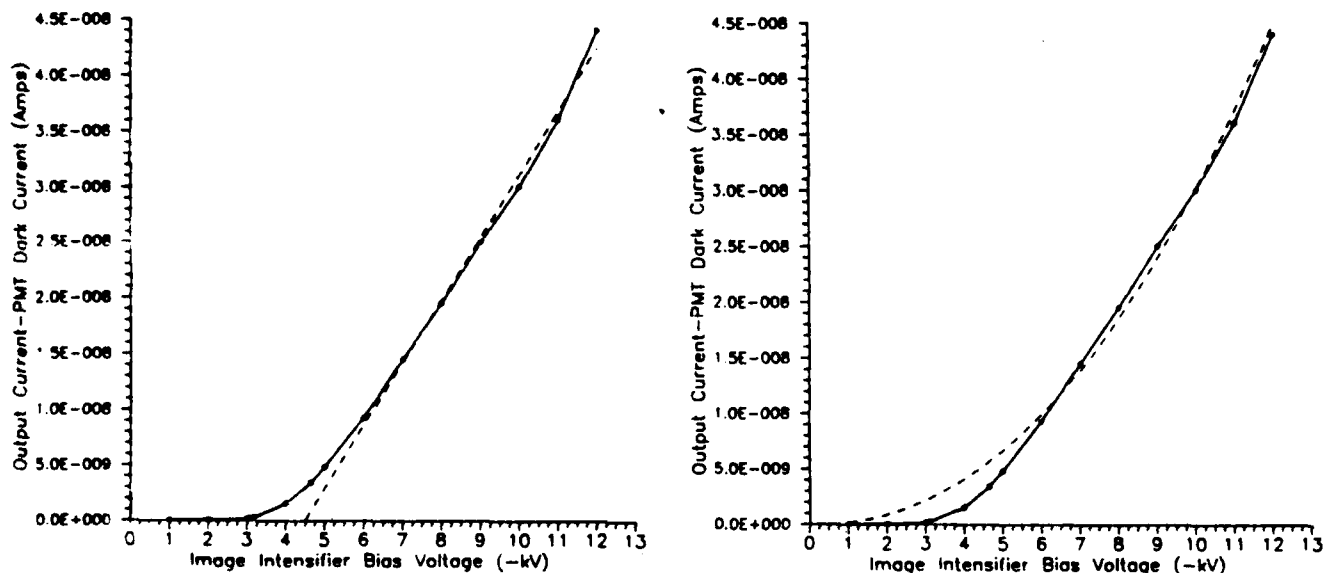


Fig. 13. Measured output of Varo image intensifier vs bias voltage with LED on: a) with a linear fit, b) with a power fit.

Extrapolating from the "LED on" curve in Fig. 12 down to the x-axis suggests a dead voltage of around -2kV (rather than the -4kV quoted by Varo). Furthermore, the portion of the curve which is emphasized by dashes suggests a value of 2.18 for n however the curve for "LED off" is completely different. On the other hand, the linear plot in Fig. 13a gives a dead voltage of -4.4kV. However, it is not clear whether a linear fit (Fig. 13a) or a power fit (Fig. 13b) should be used to best fit the data above -6kV. Therefore, it is not clear at this time what the correct dead voltage of the Varo image intensifier is.

Furthermore, it is not easy to understand why the curves in Fig. 12 for "LED on" and "LED off" are not "parallel." As is known from our own experience with PMTs,⁹ dark and signal anode currents have practically the same dependence on the applied voltage. Both represent the voltage dependence of the gain and we would have expected no different for the intensifier's gain.

Looking at Fig. 13, we see a more traditional graph of output current (proportional to the number of photons leaving the phosphor) to bias voltage on a linear plot. From zero to -3 kV, we see no output from the tube and, by drawing a straight line through the remainder of the graph, we can estimate a dead voltage of about -4.4 kV. This value is a little high compared to information supplied by Varo, which claims a dead voltage of -4 kV. As explained above, until this bias voltage is reached, photoelectrons leaving the

photocathode do not have sufficient energy to traverse the aluminized screen and excite the phosphor. From -6 to -10 kV bias, the response follows a straight line, as one would expect if $n=1$, and above -10 kV, we see that the tube output is increasing in a slightly nonlinear manner which could indicate the field emission point described above.

References

1. Green, Sam, Ph.D., McDonnell-Douglas Corporation, private communication
2. Engstrom, Ralph W., Ph.D., RCA Photomultiplier Handbook, pg. 20, RCA Corporation, Lancaster, Pennsylvania, 1980.
3. Bar-Lev, Adir, Semiconductors and Electronic Devices, 2nd ed., pg. 447, Prentice Hall, New Jersey, 1984.
4. See reference 2.
5. Final Report for Contract #N66001-85-C-0118 to Naval Ocean Systems Center, University of Arizona, Optical Sciences Center, February, 1987.
6. RCA 8852 Photomultiplier Specifications Sheet, RCA Corporation, Lancaster, Pennsylvania.
7. Kazan, B. and M. Knoll, Electronic Image Storage, pg. 87, Academic Press, New York, 1968.
8. Ibid.
9. Roehrig, Hans, Ph.D., private communication

**END
DATE
FILMED**

12-8-87